Evaluating the Therapeutic Potential and the Suitability of Neutron Beams Designed for Clinical BNCT

Ian Postuma (ian.postuma@gmail.com)
INFN Sezione di Pavia https://orcid.org/0000-0001-9678-9277
Sara Gonzalez
CNEA
Maria Herrera
CONICET
Lucas Provenzano
CNEA
Michele Ferrarini
CNAO
Chiara Magni
UNIPV
Nicoletta Protti
UNIPV
Fatemi Setareh
INFN
Valerio Vercesi
INFN
Giuseppe Battistoni
INFN
Umberto Anselmi Tambur1ni
UNIPV
Yuan Hao Liu
Neuboron
Leena Kankaanranta
Helsinki University
Hanna Koivunoro
Neutron Therapeutics
Saverio Altieri
UNIPV
Silva Bortolussi

Research

Keywords: BNCT BSA, UTCP, Epithermal neutron beam, Radiobiological figure of merit, out-of-beam dosimetry

Posted Date: October 28th, 2020

DOI: https://doi.org/10.21203/rs.3.rs-96688/v1

Journal of Radiation Oncology Informatics

Evaluating the therapeutic potential and the suitability of neutron beams designed for clinical BNCT

Research Article

Ian Postuma [1] *, Sara J González [2,3] Maria S Herrera [3] Lucas Provenzano [2,3] Michele Ferrarini [4] Chiara Magni [1,5] Nicoletta Protti [1,5] Setareh Fatemi [1] Valerio Vercesi [1] Giuseppe Battistoni [6] Umberto Anselmi Tamburini [1,9] Yuan Hao Liu [7,8] Leena Kankaanranta [10] Hanna Koivunoro [11] Saveio Altieri [1,5] Silva Bortolussi [1,5]

1 Istituto Nazionale di Fisica Nucleare (INFN), Unit of Pavia, via Bassi 6, 27100 Pavia Italy

2 Comisión Nacional de Energía Atómica, CNEA, Buenos Aires, Argentina

3 Consejo Nacional de Investigaciones Científicas y Técnicas, CONICET, Buenos Aires, Argentina

4 Centro Nazionale di Adroterapia Oncologica, CNAO, strada campeggi 53, 27100 Pavia Italy

5 University of Pavia, Department of Physics, via Bassi 6, 27100 Pavia Italy

6 Istituto Nazionale di Fisica Nucleare (INFN), Unit of Milan, via Celoria 16, 20133 Milan, Italy

7 Neuboron Medtech, Nanjing, China

8 Nanjing University of Areonautics and Astronautics, Nanjing, China

9 University of Pavia, Department of Chemistry, via Taramelli 12, 27100 Pavia Italy

10 Helsinki University Clincial Hospital, HUCH, Helsinki, Finland

11 Neutron Therapeutics, Boston, USA

* *E-mail: ian.postuma@gmail.com*

Abstract: The standard of neutron beam quality for Boron Neutron Capture Therapy (BNCT) of deep-seated tumours is currently defined by its physical characteristics in air: the epithermal neutron flux, the ratio of thermal and epithermal neutron flux, the fast neutron and photon dose contamination, and the beam collimation.
Traditionally, the beam design consists in tailoring a Beam Shaping Assembly (BSA) able to deliver a neutron beam with the recommended values of these figures of merit (FOMs).
This work investigated the possibility to produce an epithermal neutron beam able to guarantee the best clinical performance for deep-seated tumours, starting from a 5 MeV, 30 mA proton beam coupled to a beryllium target. Different Beam Shaping Assemblies were designed using those physical FOMs which, however, were not enough to establish a clear ranking of the different beams, nor to describe their clinical relevance.
To go beyond this traditional approach, beams were then evaluated employing new criteria based on the dose distributions obtained in-phantom and on the calculation of the Uncomplicated Tumour Control Probability (UTCP). Such radiobiological FOM allows establishing the therapeutic potential of the beams. Moreover, we included the concept of suitability as a criterion to select the safest BSA design, calculating the in-patient out-of-beam dosimetry.
The clinical relevance of the selected beam was finally tested in the treatment planning of a clinical case treated at the FiR 1 beam in Finland, where several patients have safely and successfully received BNCT in the last years. Despite the selected beam does not comply with all the standard physical recommendations, it shows a therapeutic potential comparable and even better than that of FiR 1. This confirms that establishing the performance of a beam cannot rely only on its physical characteristics, but requires additional criteria able to predict the clinical outcome of a BNCT treatment.

J Rad Onc Inform 2014 X(X): XX-XX

doi: 10.5166/jroi-X-X-XX

Authors have no conflicts to disclose.

Keywords: BNCT BSA • UTCP • Epithermal neutron beam • Radiobiological figure of merit • out-of-beam dosimetry

1. Introduction

Boron Neutron Capture Therapy (BNCT) is a form of hadrontherapy that exploits the products of neutron capture reactions in ^{10}B to treat neoplasms. The therapy is performed by targeting the tumour with a drug loaded with ^{10}B and subsequently irradiating the volume with a thermal neutron field (i.e. 25 meV neutrons). At this energy, the thermal neutron capture reaction $^{10}B(n,\alpha)^{7}Li$ has a high cross section (3837 b) and generates two high-LET, short-range charged particles, whose damage is localised in the proximity of cells that uptake ^{10}B. If boron concentration is sufficiently higher in the malignancy than in the normal tissues, it is possible to cause a selective lethal effect in tumour. The selectivity warranted by the biological distribution of boron makes BNCT a potential therapeutic option for disseminated or infiltrated neoplasms. Moreover, as the effect is due to highly biological effective radiation, BNCT is studied to treat recurrent or radio-resistant tumours. Many BNCT clinical trials have been performed worldwide with promising results, especially on head and neck cancer, cutaneous melanoma and brain tumours [1–3].

BNCT has been applied in institutions equipped with research nuclear reactors, which are neutron sources intense enough to ensure acceptable treatment times. Today neutron fluxes of the order of 10^{9} cm^{-2} s^{-1} can be produced with proton accelerators coupled with Be or Li targets (accelerator-based BNCT or ab-BNCT) [4]. Accelerators are more compact than reactors, easier to operate and maintain, and have no social acceptability issues, allowing their installation in health-care environments. This technology is giving a worldwide boost to new BNCT clinical

facilities. Cyclotrons for BNCT are already in use for clinical trials in two centres in Japan [5]. Other accelerators, electrostatic or Radio Frequency Quadrupole (RFQ), are being developed and installed in Argentina, Japan, Russia, Finland, USA, UK, Israel [6–12].

The Italian National Institute of Nuclear Physics (INFN) designed and constructed an RFQ proton accelerator delivering a 5 MeV, 30 mA proton beam in Continuous Wave (CW) mode [13]. The neutron yield at the Be target is 10^{14} s^{-1} with maximum neutron energy around 3.2 MeV [14]. This spectrum must be tailored for BNCT, acting on moderation and collimation.

The optimal neutron beam for BNCT of deep-seated tumours has a spectrum peaked between 1 and 10 keV [15–17], requiring a Beam Shaping Assembly (BSA) to decrease neutron energy and to collimate the beam to minimize out-of-beam dose. The BSA is a typical element of the BNCT equipment, both for accelerators and reactors, and its characteristics depend on the initial neutron energy distribution (i.e. on the type of target and on the projectile energy) in the accelerator case. Presently, there is an increasing research work designing BSAs for ab-BNCT [12, 14, 18–25]. Hence, methods to compare and evaluate simulated beams are currently under discussion, introducing new simulation instruments, computational strategies and analysis criteria.

IAEA published the TecDoc-1223 in 2001 [26] describing the desired characteristics of the neutron beams for BNCT: values had been indicated for the minimum epithermal neutron flux, the minimum degree of collimation and the maximum gamma, thermal and fast neutron contamination in air (Table 1). Together with some in-phantom quantities [27], these FOMs until now have been the only guidelines to evaluate the suitability of neutron beams for BNCT. Presently, the idea is taking shape that a neutron beam should rather be evaluated using treatment planning calculations in real clinical cases for a reliable performance evaluation: beams that do not comply with the IAEA guidelines can still be effective for some tumours. Furthermore, a neutron beam for BNCT must also follow other important criteria: it must be safe for the whole body of the patient, and it must be tested for the radio-protection limitations according to the regulations in each country. In literature, few examples of more refined computational evaluations are available [28, 29].

Beam parameter	Recommended value
Epithermal Flux (ϕ_{epi})	$> 10^{9}$ cm^{-2} s^{-1}
$\frac{\dot{D}_{fast}}{\phi_{epi}}$	$< 2.0 \cdot 10^{-13}$ cm^{-2} Gy
$\frac{\phi_{th}}{\phi_{epi}}$	< 0.05
$\frac{\dot{D}_{\gamma}}{\phi_{epi}}$	$< 2.0 \cdot 10^{-13}$ cm^{-2} Gy
$\frac{J}{\phi_{epi}}$	> 0.7

Table 1. IAEA recommendations on beam quality. The suffix *epi* refers to energy range between 0.5 eV and 10 keV.

In this work, beams obtained with different BSA configurations have been first evaluated according to the classic IAEA FOMs. For a more significant analysis, we then exploited a radiobiological figure of merit capable of classifying the beams according to their clinical performance. The same beams were then tested on a human

whole-body phantom to evaluate the dose delivered to peripheral organs. The information retrieved from these evaluations led to the selection of the best BSA configuration. The candidate beam was finally used to simulate a treatment plan in a patient bearing head and neck tumour, one of the most promising targets in present BNCT clinical trials. The result of the radiobiological figure of merit in the treatment planning was compared with that of the original BNCT treatment.

The results of this set of evaluations show that free-beam, in-air parameters are unable to provide a clear ranking of the beams performance. To define the most adequate configuration other criteria are needed, more suitable for predicting the clinical outcome of a treatment, which is the relevant goal when designing a clinical facility.

2. Materials and Methods

Presently many reactor and accelerator-based neutron sources are available, all with characteristic neutron spectra, needing ad hoc BSA materials and geometrical configuration. For the INFN RFQ accelerator (5 MeV protons on Be target), the most performing moderating material has been proved to be aluminium fluoride (AlF_3) [30], which is available only in powder. To obtain a mechanically stable BSA, a dedicated study was carried out in Pavia to densify powders of AlF_3, added with LiF. An innovative sintering process has been devised and a dedicated machine has been designed and constructed, able to obtain, for the first time, aluminium fluoride elements with nearly 100% density, showing very good mechanical properties and resistance to radiation. AlF_3 doped with LiF is used throughout this work as the bulk moderation unit, to control the epithermal neutron flux and to lower as much as possible the fast (> 10 keV) and thermal (< 0.5 eV) neutron contamination. For simplicity, we do not present all the tested BSA materials and geometrical configurations. Instead, only five set-ups are reported to show the use of a radiobiological FOM as a criterion to select the most performing BSA.

2.1. BSA material and geometrical composition

Figure 1 shows the geometrical configurations used for this work. The geometrical set-up shown in Figure 1a has a reflector (black) that embeds the bulk moderating material (grey) which is subsequently embedded into shield 1, aimed at decreasing contamination. In the second set-up, Figure 1b, the bulk material embeds the target region, to guide neutrons with the desired energy towards the beam-port, while the reflecting material separates shield 2 from the bulk material. This buffer area prevents thermal neutrons from scattering in shield 2 back into the bulk material. At the same time, epithermal neutrons escaping from the bulk material are scattered back. This BSA has a larger shield 2, to further decrease beam contamination. Finally, the configuration shown in Figure 1c is a modification of 1b, aimed at increasing lateral neutron moderation and absorption. The cone shape of 1b was reduced by increasing the amount of moderating material. To mitigate the unavoidable loss of flux, the volume of reflecting material around the bulk moderator was increased. The shape of reflector, lateral shielding and bulk moderator were optimised to reach a satisfactory epithermal neutron flux at the beam-port. The BSA in Figure 1c

was also intended to better collimate the neutron beam.

Five different beams based on these three geometrical structures were selected. Table 2 describes the material composition and geometrical set-up of these BSAs.

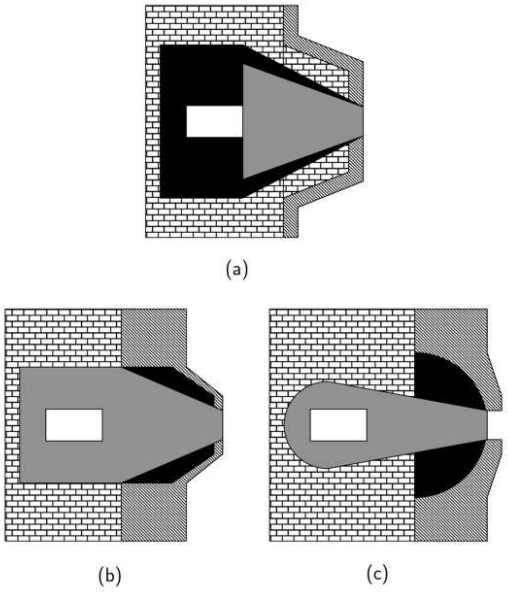

Figure 1. Schemes of the tested BSA structures. Each BSA can be separated in 4 different regions: The brick pattern is a *first shielding* material (shield 1), the black region is the *reflector*, the striped area represents a second *shielding material* (shield 2) and the grey area is the *bulk moderating material*. The central white box is the position of the target, neutrons are moderated and transported horizontally from the white box towards the beam port on the right. Lateral dimensions are 160 cm by 160 cm, for the horizontal extension refer to Table 2. The neutron source is located inside the white rectangle at the centre of the BSA and the proton beam is perpendicular to the direction of the neutron beam.

BSA	Shield 1	Shield 2	Reflector	Bulk material composition (thickness [cm])	Design
#1	Pb	HW + CLi	Pb	AlF_3 (35.5) + LiF (1) + Bi (.5) + Ti (1)	1b
#2	Pb	C + CH_2Li	Pb	AlF_3 (35.5) + LiF (1) + Bi (.5) + Ti (1)	1a
#3	Pb	C + CLi + CH_2Li + LiF	Pb + LiF	AlF_3 (35.75) + LiF (1.5) + Bi (.5) + Ti (1)	1b
#4	Pb	C + CLi	Pb	AlF_3 (35.5) + LiF (1) + Bi (.5) + Ti (1)	1b
#5	Pb	LiF + Teflon	CH_2Li	AlF_3 with 3% mass of LiF (37)	1c

Table 2. Materials and design of some tested BSA setup. The last column refers to the BSA designs shown in Figure 1

2.2. Evaluation of physical in-air parameters

The described beams were tested against the Figures Of Merit (FOM) suggested by IAEA. Values of the FOMs were obtained by transporting neutrons with MCNP6 [31] from the beryllium target through the BSA to the beam port, where a surface tally with 6 cm radius was computed for the total neutron current (F1 tally type), epithermal neutron flux (F2 tally type), thermal neutron flux, fast neutron and gamma dose (F2 tally type combined with an FM card with appropriate tissue kerma factors).

2.3. Evaluation of the therapeutic potential of beams by a radiobiological FOM

To introduce a criterion predicting the treatment outcome, we tested the beams in a phantom representing a human neck bearing a tumour. Head and neck (H&N) cancer is presently the principal target of clinical BNCT: promising clinical results have been obtained with reactors and BNCT trials for these tumours are ongoing at ab-BNCT facilities in Japan [1, 5]. The phantom is a cylinder (radius of 10 cm and height of 24 cm) of mucosa, which is the tissue at risk in H&N BNCT treatments. A 2 cm radius sphere centred 3 cm from the phantom equator surface represents the tumour. Boron concentration was assumed to be the standard in Finland treatments: 15 ppm in blood, which results in 30 ppm in mucosa and 52.5 ppm in tumour [32].

Figure 2. 3D view of the phantom simulated in front of the beam port, facing the neutron beam with the tumour region.

Figure 2 shows the simulated set-up, where the phantom is irradiated with a beam-to-phantom distance of 7.5 cm, reproducing the average distance of patients from the beam port in clinical experience [33]. The dose was calculated with the photon iso-effective model [34]. To assess the therapeutic potential, we calculated the Uncomplicated Tumour Control Probability (UTCP) [33], defined as the probability to control the tumour without complication in the relevant healthy tissue, in this case, mucosa. UTCP is the product of the tumour Control Probability (TCP) and the complementary of Normal Tissue Complication Probability (1-NTCP). The closer this FOM is to 1, the highest is the probability to control the tumour without normal tissue complications. This criterion was used for the first time by Provenzano et al. [33] for the comparison of different clinical facilities, and it is proposed here

as a criterion to select adequate beams among different candidates. UTCP was computed using TCP model for inhomogeneous dose distribution [33] and NTCP model that can predict mucositis of grade 3 or higher (≥G3) after head and neck cancer radiotherapy with photons and BNCT [34]. With this model, it is possible to calculate the treatment time that maximizes UTCP.

2.4. Evaluation of the beams suitability by out-of-beam dosimetry

Besides the therapeutic potential, it is critical to select the safest beam for the patient, i.e. the one delivering the lowest dose to the organs outside the irradiation field. To study this property, the beams were tested using the anthropomorphic phantom MIRD [35, 36]. Equivalent dose was calculated with the prescription of ICRP report 116 [37]: weight for photon dose is 1, for boron component is 20 and neutron dose has been weighted according to the function of energy described in the ICRP report 116. To compare the out-of-beam dose values with those found in literature, biologically weighted dose was also obtained by multiplying the different components by RBE/CBE shown in Table 3. These doses were computed with MCNP6 using F4 tally type combined with kerma factors.

Tissue	RBE_γ	RBE_n	CBE_B	^{10}B Concentration (μg/g)
Brain	1	3.2	1.3	15
Skin	1	2.5	2.5	22.5
Liver	1	3.2	4.2	15
Lung	1	3.2	1.3	15
Kidney	1	3.2	1.3	75
Bladder	1	3.2	1.3	15
Tumour	1	2.2	5.3	52.5

Table 3. **RBE and CBE factors employed to calculate biological dose in different tissues [38–40].**

Boron concentration was assumed to be 15 ppm in all the normal tissues except for the skin and kidneys, set to absorb 22.5 ppm [41] and 75 ppm, respectively. Kidneys are known to uptake a higher boron concentration than other tissues due to excretion of BPA via the urinary system: pharmacokinetics studies performed in animals and humans using fluorinated BPA and PET imaging have been analysed [42, 43]. Concentration in kidneys is high shortly after the injection of the tracer, and then it decreases after about 1 hour to a value around 5 times higher than in other normal tissues. At the same time, the concentration in bladder increases. Bio-distribution studies in a big animal model [41] treated with a protocol equal to the clinical one (350 mg/kg of BPA for 45 minutes) confirm the findings in the human studies. For this study, we thus assumed a boron concentration in kidney equal to 75 ppm. As shown in the PET images of the cited papers, a high boron concentration is expected in the urine after some time from BPA administration. However, the urinary bladder tissue absorbs a boron concentration similar to other normal tissues [44]. The dose delivered to the tissues due to the boron present in the urine is limited to the layer of urine adjacent to the organ walls with a thickness equal to the particles range, i.e. about 10

micrometres. For this reason, boron in urine was neglected in the calculation of the dose delivered to the bladder, assumed to uptake 15 ppm of boron.

The combination of therapeutic potential and suitability assessment allowed the ranking of the candidate beams, resulting in a clear selection of the best BSA design.

2.4.1. Treatment Planning simulation

The selected beam was finally used to simulate a BNCT treatment plan. The chosen clinical case is a Head and Neck cancer patient (squamous cell carcinoma) treated with BPA-mediated BNCT in Finland [32]. The performance of the selected beam is compared with that of FiR 1 in the real treatment.

Figure 3. Image a) shows a slice of the patient DICOM image segmented into 5 materials, which is then converted into a voxelized phantom by MultiCell as shown in image b). Image c) shows the TPS set-up as fed into the MCNP simulation.

MultiCell was used as the Treatment Planning System, to obtain the voxelized patient model shown in Figure 3a (segmented image) and in Figure 3b (3D representation), to set the two fractions treatment configuration and to produce the input for dose calculation by MCNP [45, 46]. Figure 3c shows the voxelized phantom positioned in front of the beam port. The dose-limiting point in mucosa used to calculate the optimum treatment time and maximum UTCP is the one selected by medical doctors in the real treatment. Based on the obtained irradiation time, photon iso-effective doses and the Dose Volume Histogram (DVH) were calculated in the contoured tumour volume. UTCP curve was computed as described by Provenzano et al [33].

3. Results

3.1. Evaluation of physical in-air parameters

Table 4 shows the results of the calculation of physical FOMs for each beam (Table 2 and Figure 1), compared to the recommended values. BSA #1 and BSA #4 ensure a lower gamma contamination while keeping a high neutron flux. This is mainly due to the use of heavy water and graphite, in shield 2 region, instead of materials containing hydrogen. BSA #2 is the one with the lowest fast neutron dose contamination, while BSA #3 is the one

with the lowest gamma dose contamination. These beams show lower fast neutron dose contamination compared to BSA #1 and BSA #4, the main reason being that the shielding material contains hydrogen, which scatters low energy neutrons back into the beam. As a result, the epithermal neutron flux increases, but the epithermal energy spectrum is shifted towards energies lower than 1 keV. BSA #5 is characterised by higher collimation (it is the only one complying with IAEA recommendation for this parameter) at the expense of lower epithermal neutron flux and the highest fast neutron dose contamination.

Table 4 shows how difficult it can be to evaluate a beam based on fixed values of physical properties. None of the tested beams is clearly optimal compared to the IAEA values. However, they may still be useful for patient treatment. To assess the suitability for clinical use, the beams were tested using the UTCP.

	ϕ_{epi}	$\frac{\phi_{th}}{\phi_{epi}}$	$\frac{\dot{D}_{Fast}}{\phi_{epi}}$	$\frac{\dot{D}_{\gamma}}{\phi_{epi}}$	$\frac{J}{\phi_{epi}}$
	10^9 (cm^{-2} s^{-1})	-	10^{-13} (cm^2 Gy)	10^{-13} (cm^2 Gy)	-
Recommended	> 1	< 0.05	< 2.0	< 2.0	> 0.7
BSA #1	2.58	0.019	9.16	3.96	0.59
BSA #2	2.56	0.054	6.70	6.66	0.60
BSA #3	1.73	0.004	7.71	2.70	0.62
BSA #4	2.79	0.018	9.09	3.78	0.59
BSA #5	1.08	0.009	9.50	4.17	0.74

Table 4. IAEA FOM calculated for the BSAs listed in Table 2. The reported results have a relative error lower than 2%.

3.1.1. Radiobiological FOM

Table 5 shows the evaluation of the UTCP on the cylindrical phantom, obtained by maximizing this FOM for each BSA configuration. With this evaluation, it is clear that BSA #5 has the highest UTCP value, obtained from the highest TCP and lowest NTCP. All beams allow reasonable treatment times. To highlight the clinical relevance of UTCP evaluation, note that the dose D (the maximum dose to the healthy tissue at risk) is very close to the clinically prescribed dose of 6 Gy [47].

BSA	T_{irr} (min)	UTCP	TCP	NTCP	D (Gy)	% Dose (n,α)	(n,p)	(n,n')	γ
#1	10	**0.41**	0.5	0.19	5.79	0.61	0.06	0.06	0.27
#2	12.5	**0.40**	0.52	0.23	6.15	0.59	0.05	0.06	0.3
#3	20	**0.44**	0.57	0.23	5.81	0.62	0.07	0.06	0.25
#4	9.5	**0.40**	0.54	0.26	5.98	0.61	0.06	0.06	0.27
#5	24.5	**0.47**	0.58	0.18	5.59	0.61	0.09	0.06	0.23

Table 5. This table shows the results of the simulations with the cylindrical phantom. Each UTCP value is followed by its TCP, NTCP and irradiation time T_{irr}. The dose column D shows the maximum dose to the healthy tissue, while the % Dose section displays the different contributions to the dose D.

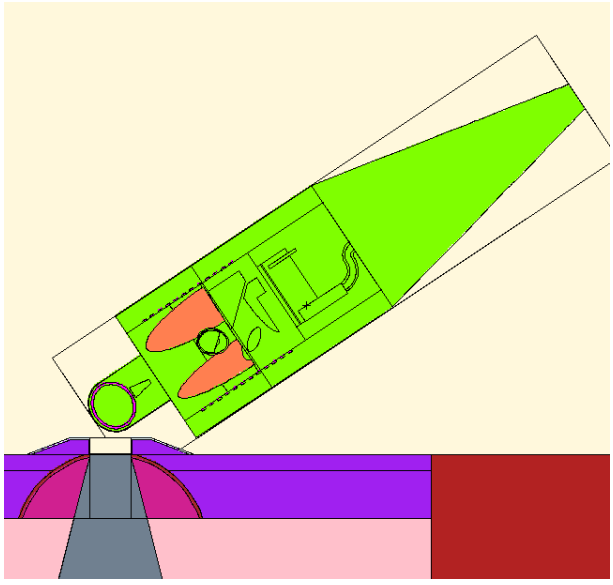

Figure 4. The image shows an MCNP plot of the MIRD phantom position that mimics a typical head irradiation in BNCT.

3.1.2. Out-of-beam dosimetry

The anthropomorphic male MIRD phantom, as shown in Figure 4 was positioned in a representative irradiation position for H&N cancer treatment. For all beams, the biological weighted dose in Gy_Eq has been calculated in all the organs of the phantom. Figure 5 shows that BSA #5 delivers doses significantly lower to the organs outside the irradiation field. In this respect, it is thus preferable.

This result together with the therapeutic potential is a clear demonstration that BSA #5 is clinically the most performing beam. Table 6 shows the dosimetry of this BSA on the organs of MIRD phantom. The values refer to the dose absorbed by a patient in a treatment time as calculated to maximise the UTCP: 24.5 minutes. The Table reports also the absorbed dose (Gy) separating the radiation components, and the weighted dose (Sv), calculated following the prescription of ICRP report 116 [48].

3.1.3. Characteristics of the selected beam

The BSA delivering BSA #5 is showed in detail in Figure 6. The neutron spectrum averaged over the beam-port area (6 cm radius circle) peaks around the desired energy of 10 keV. The flux decreases sharply when averaged over a circular ring going from 6 cm radius to 12 cm radius, the out-of-beam area (Figure 7). Figure 8 shows spectrum and flux behavior in-beam and out-of-beam. In Figure 8a, the logarithmic spectrum averaged over circular sectors of radii between 1 and 11 cm, demonstrates that the spectral distribution is maintained below 6 cm (in-beam). Out of beam, the flux decreases with the radius, and the proportion of the spectrum components changes. Figure 8b shows the distribution of the different spectral components as a function of the radius. Flux variation is within 20% inside the beam-port, and it sharply decreases out of beam. The thermal, epithermal and fast neutron components change at increasing radial distance. This is due to the different material composition of

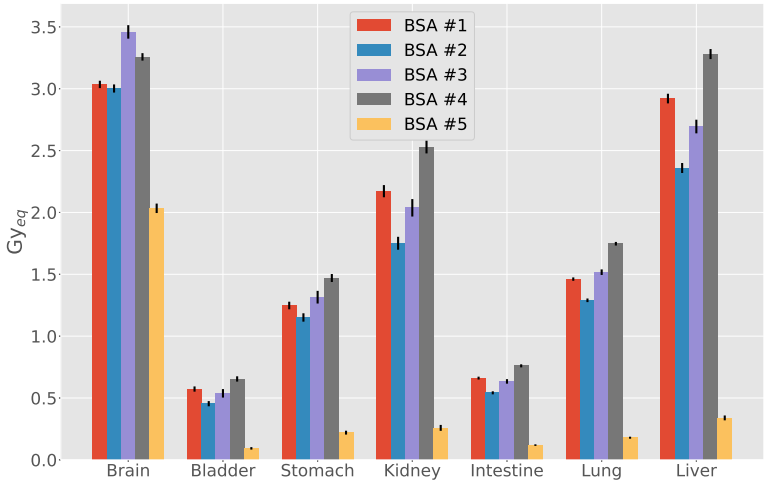

Figure 5. Comparison of out-of-beam dose evaluated in the MIRD phantom. Dose is evaluated for the treatment time, which is: 10 minutes for BSA #1, 12.5 minutes for BSA #2, 20 minutes for BSA #3, 9.5 minutes for BSA #4 and 24.5 minutes for BSA #5.

Organ	D_N (Gy)	D_B (Gy)	D_H (Gy)	D_γ (Gy)	D_W (Sv)	D_{Eq} (Gy_Eq)	Err (Gy_Eq)
Brain	1.06E-02	1.21E-02	4.14E-01	4.38E-01	5.11	2.03	0.04
Bladder	1.06E-03	1.22E-03	7.27E-04	6.35E-02	0.48	0.09	0.01
Stomach	1.51E-03	1.74E-03	9.99E-03	1.49E-01	0.77	0.22	0.02
Kidneys	1.21E-03	1.39E-03	2.99E-03	1.10E-01	2.26	0.26	0.02
Intestine	1.05E-03	1.20E-03	2.97E-03	8.29E-02	0.51	0.12	0.01
Lungs	1.88E-03	2.16E-03	2.90E-02	5.61E-03	0.80	0.18	0.01
Liver	1.33E-03	1.53E-03	7.55E-03	1.15E-01	1.12	0.34	0.02
Heart	1.87E-03	2.15E-03	2.22E-02	1.66E-01	0.95	0.28	0.02
Spleen	1.21E-03	1.40E-03	9.83E-03	1.45E-01	0.65	0.21	0.02
Head	5.51E-03	6.31E-03	1.99E-01	3.72E-01	2.82	1.15	0.02
Thyroid	4.83E-03	5.54E-03	9.14E-02	2.68E-01	2.32	0.68	0.07
Testicles	7.84E-04	9.03E-04	5.02E-04	7.12E-02	0.38	0.09	0.01
Pancreas	1.07E-03	1.24E-03	2.57E-03	9.09E-02	0.53	0.13	0.01
Pharynx	7.12E-03	8.18E-03	1.45E-01	3.36E-01	3.37	0.98	0.08
Marrow	1.45E-03	1.66E-03	4.91E-02	1.60E-01	0.80	0.35	0.01
Adrenal	9.11E-04	1.05E-03	1.04E-02	1.01E-01	0.48	0.16	0.04
Thymus	2.49E-03	2.87E-03	1.62E-02	1.77E-01	1.20	0.29	0.04
Skin	1.73E-03	1.98E-03	6.79E-02	2.06E-01	1.28	0.54	0.01
Trunk	1.43E-03	1.65E-03	1.81E-02	1.46E-01	0.74	0.24	0.00

Table 6. Absorbed dose (Gy), equivalent dose (Sv) and biologically weighted dose (Gy_Eq) to the organs of a MIRD phantom for BSA #5. Dose is evaluated considering the whole treatment time of 25.4 minutes.

the BSA: on the beam axis AlF_3 moderates the neutron spectra to a peak energy of $\approx$ 1 keV, while out of beam, the BSA contains a high concentration of hydrogen and consequently fast and epithermal neutrons are moderated towards thermal energies.

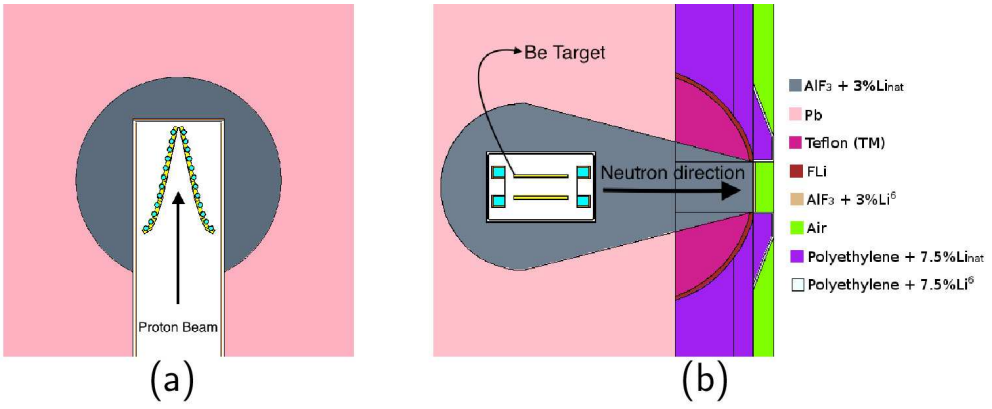

Figure 6. Geometrical configuration of the final BSA, the different colours represent the material composition of the BSA. Left: xy plane: the proton beam hits the target in the z direction. Right: xz plane. The target has a V-shape, to keep a compact design while removing the total heat generated [14].

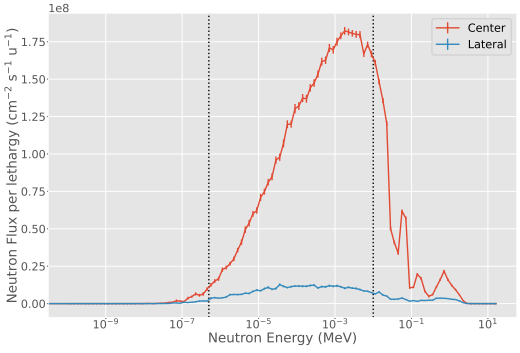

Figure 7. Final BSA energy spectra at the surface of the beam-port. Blue line: energy spectrum in a 6 cm radius disk, corresponding to the beam-port. Yellow line: spectrum in a ring with minimum radius of 6 cm and maximum radius of 12 cm. The two vertical dotted lines separate thermal from epithermal energy ranges ($5\cdot 10^{-7}$ MeV) and epithermal from fast energy ranges (10^{-2} MeV).

3.2. Treatment Planning

The results of the treatment planning simulation for the optimum irradiation time and the corresponding data for FiR 1 are shown in Table 7. Even though BSA #5 only partially satisfies the recommendations of the IAEA FoMs, the maximum UTCP is higher than the one obtain with Fir 1 (a beam that complies with all recommendations). For approximately the same NTCP, the TCP for BSA #5 is 0.56, for FiR 1 is 0.49, as shown in Figure 9. The higher TCP is a consequence of the higher minimum dose delivered to the tumour, as shown in Figure 10. In fact, BSA #5 has a higher fast component than FiR 1, thus it is more penetrating.

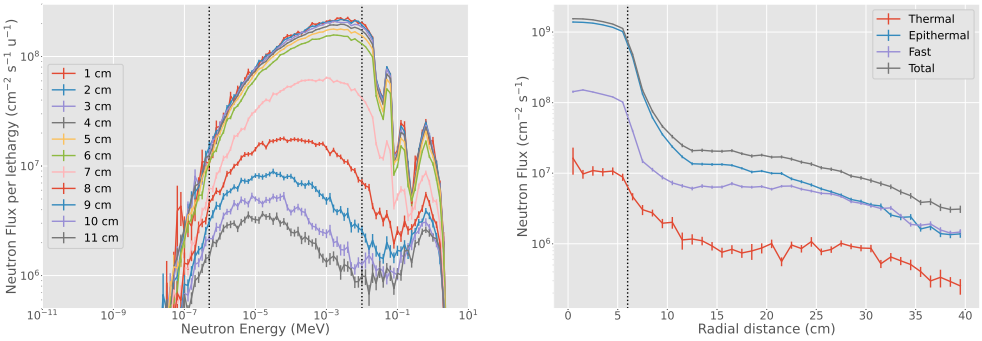

Figure 8. Neutron flux and energy spectra at the beam-port for BSA #5. a) neutron spectra in concentric rings, with radii increasing by 1 cm. The two vertical dotted lines separate thermal from epithermal energy ranges ($5\cdot 10^{-7}$ MeV) and epithermal from fast energy ranges (10^{-2} MeV). b) radial neutron flux distribution from the centre of the beam-port in concentric rings going from 0 cm to 40 cm of radius. The vertical dotted line delimits the beam-port radius. Blue: thermal neutron flux (E $\leq 5\cdot 10^{-7}$ MeV), orange: epithermal flux ($5\cdot 10^{-7}$ MeV $<$ E $\leq 10^{-2}$ MeV), green: fast flux (10^{-2} MeV $<$ E) and red: total neutron flux.

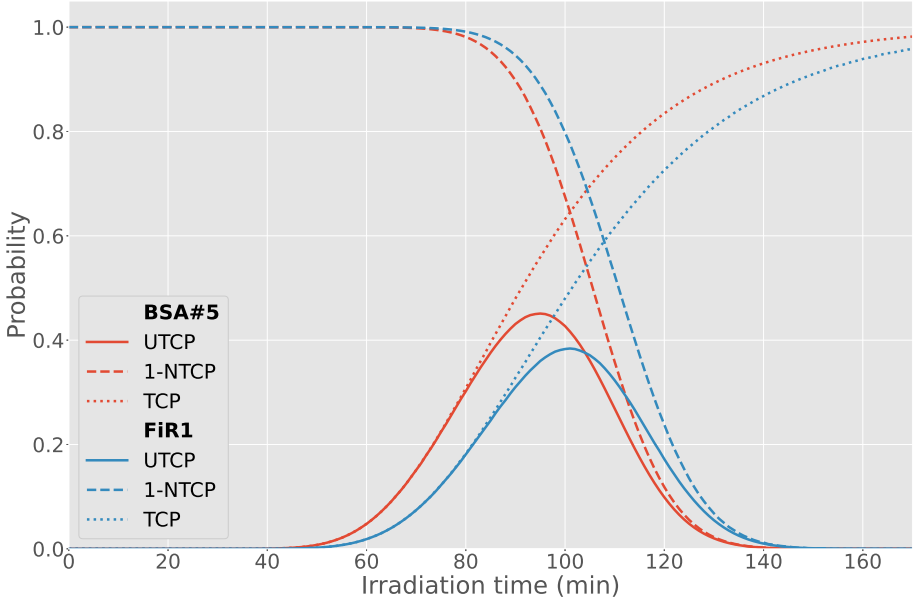

Figure 9. Comparison of the UTCP value for BSA #5 and FiR 1 as a function of the irradiation time.

4. Discussion

In designing a clinical BNCT facility based on the accelerator built by INFN, the first step was to chose the BSA generating a beam suitable to treat deep-seated tumours. The free-beam in-air parameters proved to be a

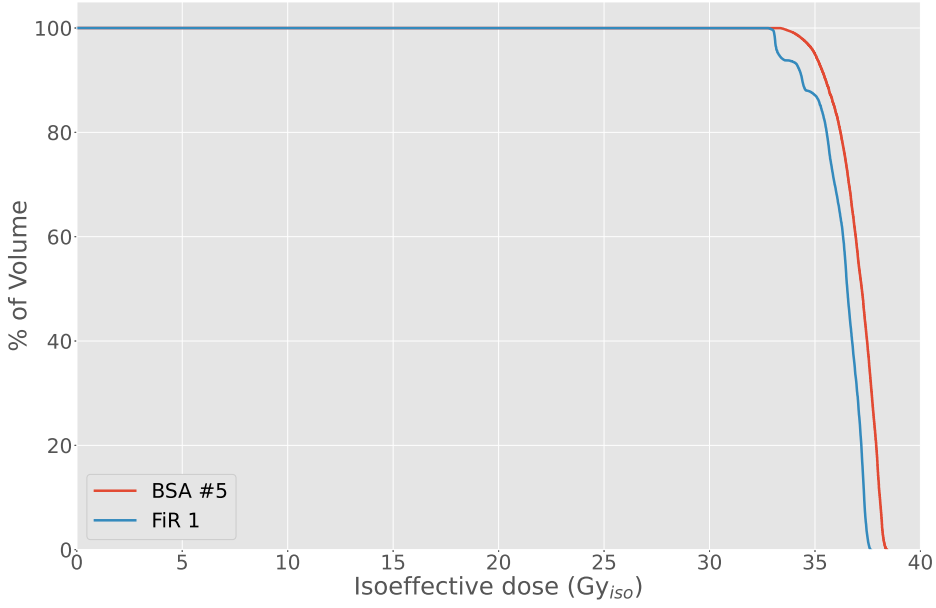

Figure 10. **Comparison of the DVH obtained with BSA #5 and FiR 1.**

Beam	T_{irr} (min)	UTCP	TCP	NTCP	D (Gy)	% Dose (n,α)	(n,p) and (n,n')	γ
BSA #5	95	**0.45**	0.56	0.19	6.0	62	8	30
FiR 1	101	**0.38**	0.49	0.22	5.4	74	6	20

Table 7. Results of the treatment planning simulation using BSA #5 and corresponding values for FiR 1 . The maximum UTCP, TCP and NTCP is reported for the optimum irradiation time T_{irr} of each beam. Dose D is the maximum absorbed dose to the dose-limiting point in healthy tissue and the % Dose displays the different contributions to the dose D.

descriptive tool which however did not allow a ranking of the candidate beams. We then introduced the concept of *therapeutic potential*, i.e. the capacity to treat a deep-seated tumour without damaging the tissue at risk. For this assessment, we evaluated the UTCP, a radiobiological FOM which condenses the 3D dose distribution into one value related to the clinical outcome. This FOM allowed a rating of the 5 candidates. UTCP is particularly interesting because it is a prediction of the clinical outcome of the irradiation. To select the safest beam for the clinical treatment, we calculated the dose delivered to the other organs of the patient. This figure describes the *suitability* of a BNCT neutron beam. It is not possible to define a threshold above which the dose absorbed in an organ is considered too high for the treatment, because the priority is the clinical outcome of the tumour irradiation. Hence, we selected the configuration ensuring the minimum out-of-beam absorbed dose. We then compared the results with those obtained in similar irradiation position with both a designed ab-BNCT beam and with a reactor beam used in BNCT clinical applications (JRR4, Japan) [28, 49]. To this end, the components of

absorbed dose were weighted using the RBE/CBE values and considering boron concentration listed in the cited documents. Figure 11 shows that the selected beam is comparable with the one designed by Herrera et al. [28], and delivers a dose to peripheral organs only slightly higher than the JRR4 beam.

Finally, we used the selected beam to compare its performance with the reference neutron facility FiR 1, in a clinical case that was successfully treated there. If clinical decision is in favour of selecting the treatment time that maximises the UTCP, the therapeutic potential of the selected beam - quantified by the maximum UTCP- is 15% higher than the one obtained for FiR 1. The real irradiation time of the H&N cancer patient treated with FiR 1 was 110 min, a value slightly higher than the one that maximises the UTCP. If we now simulate an irradiation time to equate the NTCP of the real treatment, the candidate beam achieves a TCP value 15% higher than the one obtained with FiR 1 in an irradiation time almost identical (i.e., a TCP value of 0.7 in 105 min for BSA #5 VS a TCP value of 0.6 in 110 min for FiR 1).

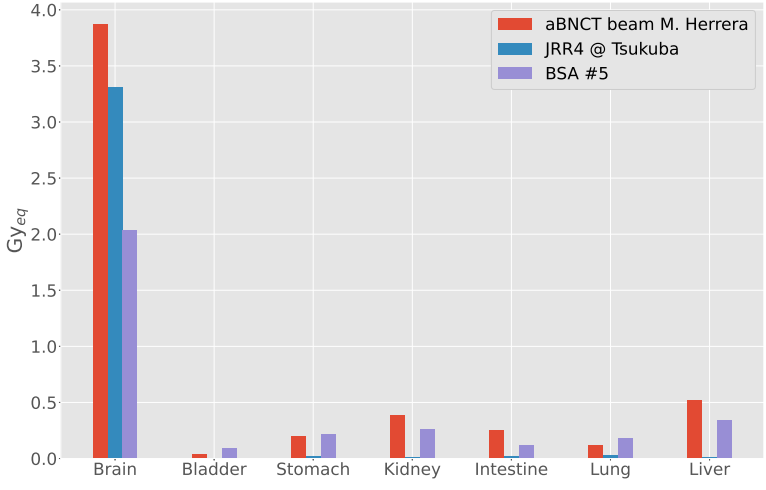

Figure 11. Out-of-beam dose evaluated in the MIRD phantom with BSA #5, with a clinical reactor beam (JRR4) and with the ab-BNCT neutron beam designed by Herrera starting for 2.7 MeV protons coupled with Li target [49].

5. Conclusions

The results obtained in this work confirm that it is possible to produce a neutron beam for clinical BNCT from the INFN RFQ, which accelerates a 5 MeV, 30 mA proton beam on a Be target. The described optimisation allowed selecting an appropriate beam for clinical BNCT. The final beam satisfies only some of the IAEA recommendations. However, it proved to ensure a comparable clinical performance to that of our reference beam FiR 1 for H&N treatment.

This work proposes a comprehensive method to adequately evaluate the *therapeutic potential* and the *suitability* of BNCT beams. Our approach adds to the standard evaluation of the in-air physical parameters, the calculation of suitable radiobiological FOMs and out-of-field dose that directly account for the clinical performance and safety of these beams. An important discussion is now ongoing within the BNCT community on the necessity to establish common guidelines to evaluate BNCT beams. This is a non-trivial issue because the evaluation criteria strictly depend on the type of tumours that are addressed, i.e. shallow or deep-seated, and thus on the spectra that are preferable. Nevertheless, the biological effects of the overall dose distributions in patient must be taken into account. For this reason, radiobiological figures of merit such as TCP, NTCP and UTCP, give a deeper insight into the clinical effectiveness and outcome of the simulated treatment planning thus providing a robust criterion to predict the beam performance.

List of abbreviations

1. BNCT: Boron Neutron Capture Therapy
2. IAEA: International Atomic Energy Agency
3. TCP: Tumour Control Probability
4. NTCP: Normal Tissue Complication Probability
5. UTCP: Uncomplicated Tumour Control Probability
6. FOM: Figure Of Merit
7. RFQ: Radio Frequency Quadrupole
8. INFN: Istituto Nazionale di Fisica Nucleare
9. BSA: Beam Shaping Assembly

Athical approval and consent to participate

Not applicable

Consent for publication

Not applicable

Availability of supporting data

Not applicable

Competing Interests

No competing interests

Fundings

Ministero degli affari esteri e della cooperazione internazionale (MAECI) grant PGR00710

Author contributions

IP adapted the neutron source in the beryllium target and validated it using experimental results; performed the simulations on BSA proposing all the described configurations; made the evaluations necessary to select the best beams (in air, in phantom). He wrote the manuscript (together with SB). SJG guided the treatment planning model and the discussion about the criteria to be used to improve the evaluation method. MSH started a deeper analysis of a simulated beam and proposed new figures of merit used in this work. LP helped in the treatment planning calculations. MF is expert in radioprotection and guided the development of beam #5. CM performed the radioprotection dosimetric study in the air of the irradiation room. NP and SF collaborated to the discussion about the dosimetry and the radiation background around the irradiation position. VV and GB participated in the scientific discussion and helped with reviewing the written English. UAT developed the bulk moderating material which characterises the main moderating material in the simulations. Y-HL participated in the discussion about the new figures of merit to be used to better evaluated the designed beam. LK and HK shared the BNCT clinical case and participated in the evaluation of the TP simulations. SA participated in the study design and reviewed the results. SB supervised this work, contributed to the study design, helped in the treatment planning calculation, guided the advancements of the work and the optimisation of the beam according to the different chosen criteria, wrote the manuscript (together with IP).

Acknowledgements

This work has been carried out in the frame of INFN project BEAT_PRO, and in the NEU_BEAT project, funded by Italian Ministry of Foreign Affairs and International Cooperation in the 2016-2018 scheme of the Scientific and Technological Cooperation Agreement between Italy and China.

6. References

References

[1] Koivunoro H, Kankaanranta L, Seppälä T, Haapaniemi A, Mäkitie A and Joensuu H 2019 *Radiotherapy and Oncology* **137** 153 – 158

[2] Menéndez P, Pereira M, Casal M, González S, Feld D, Santa Cruz G, Kessler J, Longhino J, Blaumann H, Rebagliati R J *et al.* 2009 *Applied Radiation and Isotopes* **67** S50–S53

[3] Lan T L, Chou F I, Lin K H, Pan P S, Lee J C, Huang W S, Liu Y M, Chao Y and Chen Y W 2020 *Applied Radiation and Isotopes* **160** 109105

[4] Rassow J and Sauerwein W 2012 Prescribing, recording and reporting of bnct *Neutron Capture Therapy* ed Sauerwein W, Wittig A, Moss R and Nakagawa Y (Springer Berlin Heidelberg) pp 277–285 ISBN 978-3-642-31333-2

[5] Suzuki M 2019 *International journal of clinical oncology* 1–8

[6] Kreiner A, Vento V T, Levinas P, Bergueiro J, Di Paolo H, Burlon A, Kesque J, Valda A, Debray M, Somacal H *et al.* 2009 *Applied Radiation and Isotopes* **67** S266–S269

[7] Kumada H, Matsumura A and Sakurai H 2011 New challenge for advanced bnct in university of tsukuba. in the front edge of bnct development *Proceedings of Sixth Young Researchers BNCT Meeting* pp 132–136

[8] Aleynik V, Burdakov A, Davydenko V, Ivanov A, Kanygin V, Kuznetsov A, Makarov A, Sorokin I and Taskaev S 2011 *Applied Radiation and Isotopes* **69** 1635–1638

[9] Savolainen S, Kortesniemi M, Timonen M, Reijonen V, Kuusela L, Uusi-Simola J, Salli E, Koivunoro H, Seppälä T, Lönnroth N *et al.* 2013 *Physica Medica* **29** 233–248

[10] Kwan J, Anderson O, Reginato L, Vella M and Yu S 1995 *Nuclear Instruments and Methods in Physics Research Section B: Beam Interactions with Materials and Atoms* **99** 710–712

[11] Allen D A, Beynon T D, Green S and James N D 1999 *Medical Physics* **26** 77–82

[12] Halfon S, Paul M, Arenshtam A, Berkovits D, Bisyakoev M, Eliyahu I, Feinberg G, Hazenshprung N, Kijel D, Nagler A *et al.* 2011 *Applied Radiation and Isotopes* **69** 1654–1656

[13] Mathot S 2004 *LNL TRASCO-note*

[14] Esposito J, Colautti P, Fabritsiev S, Gervash A, Giniyatulin R, Lomasov V, Makhankov A, Mazul I, Pisent A, Pokrovsky A *et al.* 2009 *Applied Radiation and Isotopes* **67** S270–S273

[15] Farías R O, Bortolussi S, Menéndez P R and González S J 2014 *Physica Medica* **30** 888–897

[16] Yanch J C, Zhou X L and Brownell G L 1991 *Radiation Research* **126** 1–20

[17] Bisceglie E, Colangelo P, Colonna N, Santorelli P and Variale V 2000 *Physics in Medicine and Biology* **45** 49

[18] Wang C K C and Moore B R 1994 *Medical Physics* **21** 1633–1638

[19] Allen D and Beynon T 1995 *Physics in Medicine and Biology* **40** 807

[20] Blackburn B W, Yanch J C and Klinkowstein R E 1998 *Medical Physics* **25** 1967–1974

[21] Lee C and Zhou X L 1999 *Nuclear Instruments and Methods in Physics Research Section B: Beam Interactions with Materials and Atoms* **152** 1–11

[22] Howard W, Grimes S, Massey T, Al-Quraishi S, Jacobs D, Brient C and Yanch J 2001 *Nuclear Science and*

Engineering **138** 145–160

[23] Burlon A, Kreiner A, Valda A, Minsky D, Somacal H, Debray M and Stoliar P 2005 *Nuclear Instruments and Methods in Physics Research Section B: Beam Interactions with Materials and Atoms* **229** 144–156

[24] Kobayashi T, Bengua G, Tanaka K and Nakagawa Y 2007 *Physics in Medicine and Biology* **52** 645

[25] Ceballos C, Esposito J, Agosteo S, Colautti P, Conte V, Moro D and Pola A 2011 *Applied Radiation and Isotopes* **69** 1660–1663

[26] Rorer D, Wambersie G, Whitmore G, Zamenhof R, Levin V, Andreo P and Dodd D 2001 *IAEA, 2001 (8)* 75–77

[27] Sakamoto S, Kiger III W and Harling O 1999 *Medical Physics* **26** 1979–1988

[28] Herrera M, González S, Minsky D and Kreiner A 2013 *Physica Medica* **29** 436–446

[29] Capoulat M and Kreiner A 2016 *Physica Medica*

[30] IPostuma 2016 *Clinical application of accelerator-based Boron Neutron Capture Therapy: optimisation of procedures, tailoring of a neutron beam and evaluation of its dosimetric performance.* Ph.D. thesis University of Pavia

[31] Goorley T, James M, Booth T, Brown F, Bull J, Cox L J, Durkee J, Elson J, Fensin M, Forster R A, Hendricks J, Hughes H G, Johns R, Kiedrowski B, Martz R, Mashnik S, McKinney G, Pelowitz D, Prael R, Sweezy J, Waters L, Wilcox T and Zukaitis T 2012 *Nuclear Technology* **180** 298–315

[32] Kankaanranta L, Seppälä T, Koivunoro H, Saarilahti K, Atula T, Collan J, Salli E, Kortesniemi M, Uusi-Simola J, Välimäki P, Mäkitie A, Seppänen M, Minn H, Revitzer H, Kouri M, Kotiluoto P, Seren T, Auterinen I, Savolainen S and Joensuu H 2012 *International Journal of Radiation Oncology*Biology*Physics* **82** e67 – e75

[33] Provenzano L, Koivunoro H, Postuma I, Longhino J, Boggio E, Farías R, Bortolussi S and González S 2019 *Physica Medica* **67** 9 – 19 ISSN 1120-1797

[34] González S J, Pozzi E C C, Hughes A M, Provenzano L, Koivunoro H, Carando D G, Thorp S I, Casal M R, Bortolussi S, Trivillin V A, Garabalino M A, Curotto P, Heber E M, Cruz G A S, Kankaanranta L, Joensuu H and Schwint A E 2017 *Physics in Medicine & Biology* **62** 7938–7958

[35] Eckerman K, Cristy M and Ryman J 1996 *Oak Ridge, TN: Oak Ridge National Laboratory*

[36] Krstić D and Nikezić D 2007 *Computer Physics Communications* **176** 33–37

[37] ICRP I 2010 *Conversion Coefficients for Radiological Protection Quantities for External Radiation Exposures*

[38] Suzuki M, Masunaga S I, Kinashi Y, Takagaki M, Sakurai Y, Kobayashi T and Ono K 2000 *Cancer Science* **91** 1058–1064

[39] Coderre J A, Turcotte J C, Riley K J, Binns P J, Harling O K and Kiger W 2003 *Technology in cancer research & treatment* **2** 355–375

[40] Kiger J L, Kiger III W S, Riley K J, Binns P J, Patel H, Hopewell J W, Harling O K, Busse P M and Coderre J A 2008 *Radiation research* **170** 60–69

[41] Farías R, Garabalino M, Ferraris S, Santa María J, Rovati O, Lange F, Trivillin V, Monti Hughes A, Pozzi E,

Thorp S *et al.* 2015 *Medical Physics* **42** 4161–4173

[42] Hanaoka K, Watabe T, Naka S, Kanai Y, Ikeda H, Horitsugi G, Kato H, Isohashi K, Shimosegawa E and J H 2014 *EJNMMI Res* **4** 70

[43] Shimosegawa E, Isohashi K, Naka S, Horitsugi G and J H 2016 *Ann Nucl Med* **30** 749

[44] Kono Y, Kurihara H, Kawamoto H, Yasui N, Honda N, Igaki H and Itami J 2017 *Acta Radiologica* **58** 1094–1100

[45] Farias R O and González S J 2012 *Proceedings of the 15th international congress on neutron capture therapy, Tsukuba, Japan* 148–150

[46] Farias R O 2015 *Dosimetría y modelado computacional para irradiaciones extracorpóreas en humanos en el marco de la Terapia por Captura Neutrónica en Boro - PhD thesis - Buenos Aires, Argentina* Ph.D. thesis Universidad Nacional de General San Martin, Comision Nacional de Energia Atomica, Istituto de Tecnologia

[47] H K 2012 *Dosimetry and dose planning in boron neutron capture therapy: Monte Carlo studies* Ph.D. thesis University of Helsinki

[48] Petoussi-Henss N, Bolch W, Eckerman K, Endo A, Hertel N, Hunt J, Pelliccioni M, Schlattl H and Zankl M 2010 *Annals of the ICRP* **40** 1–257

[49] Herrera M 2014 *Simulación computacional de la producción de flujos neutrónicos y planificación de tratamiento para la Terapia por Captura Neutrónica en Boro con aceleradores* Ph.D. thesis Universidad Nacional de General San Martin, Comision Nacional de Energia Atomica, Istituto de Tecnologia

Figures

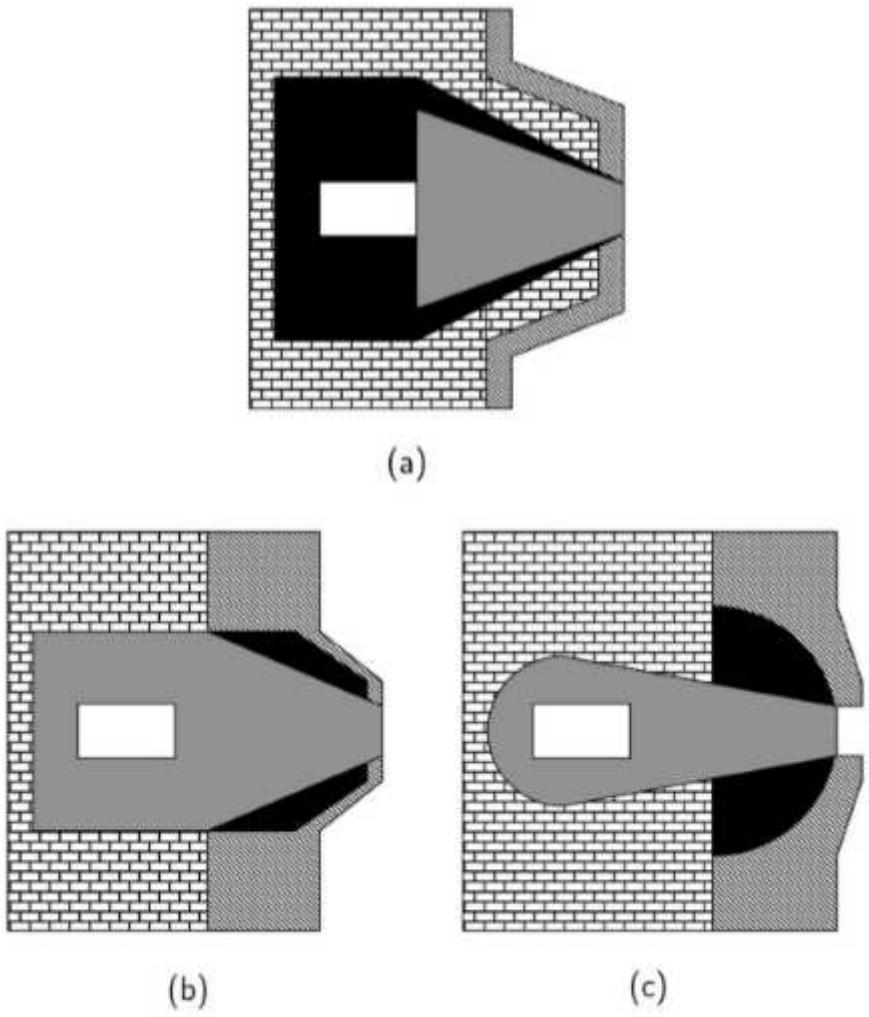

Figure 1

Schemes of the tested BSA structures. Each BSA can be separated in 4 different regions: The brick pattern is a first shielding material (shield 1), the black region is the reflector, the striped area represents a second shielding material (shield 2) and the grey area is the bulk moderating material. The central white box is the position of the target, neutrons are moderated and transported horizontally from the white box towards the beam port on the right. Lateral dimensions are 160 cm by 160 cm, for the horizontal extension refer to Table 2. The neutron source is located inside the white rectangle at the centre of the BSA and the proton beam is perpendicular to the direction of the neutron beam.

Figure 2

3D view of the phantom simulated in front of the beam port, facing the neutron beam with the tumour region.

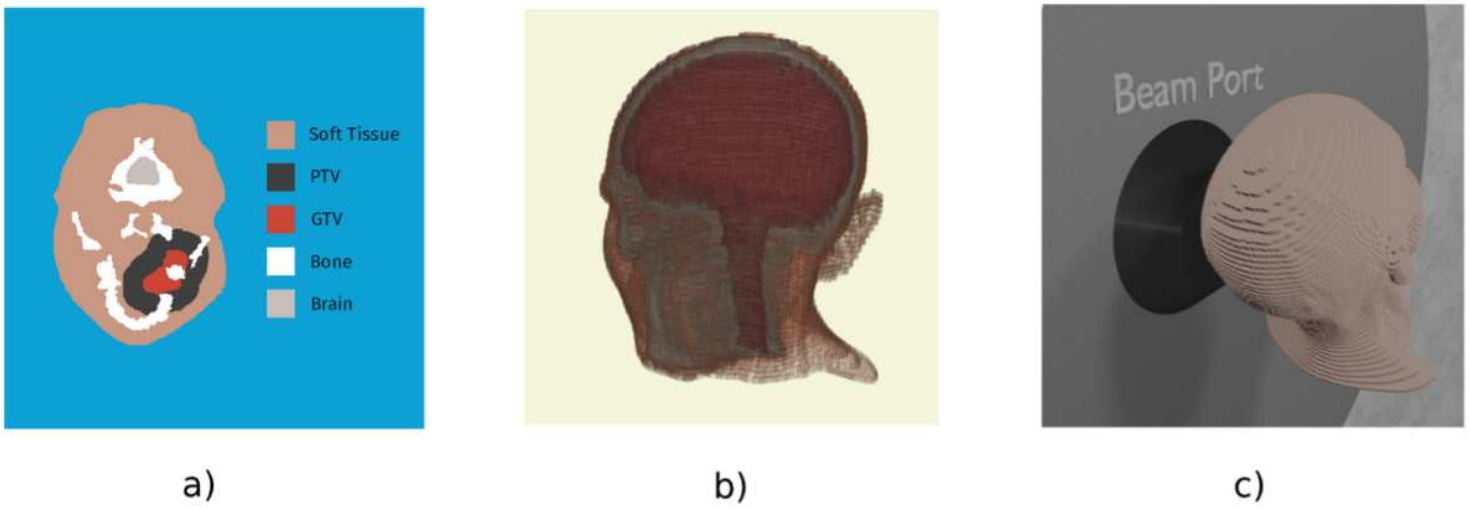

Figure 3

Image a) shows a slice of the patient DICOM image segmented into 5 materials, which is then converted into a voxelized phantom by MultiCell as shown in image b). Image c) shows the TPS set-up as fed into the MCNP simulation.

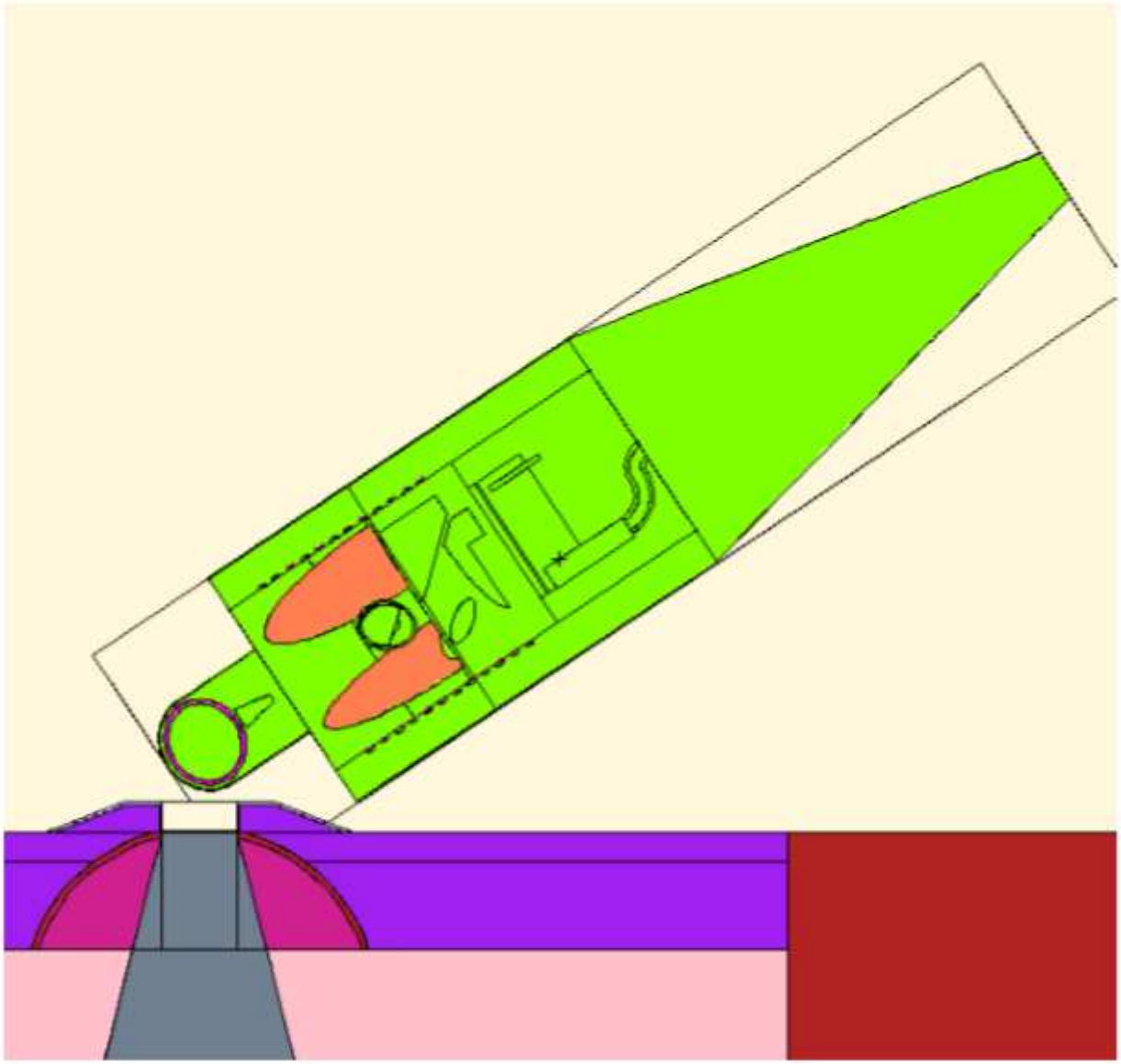

Figure 4

The image shows an MCNP plot of the MIRD phantom position that mimics a typical head irradiation in BNCT.

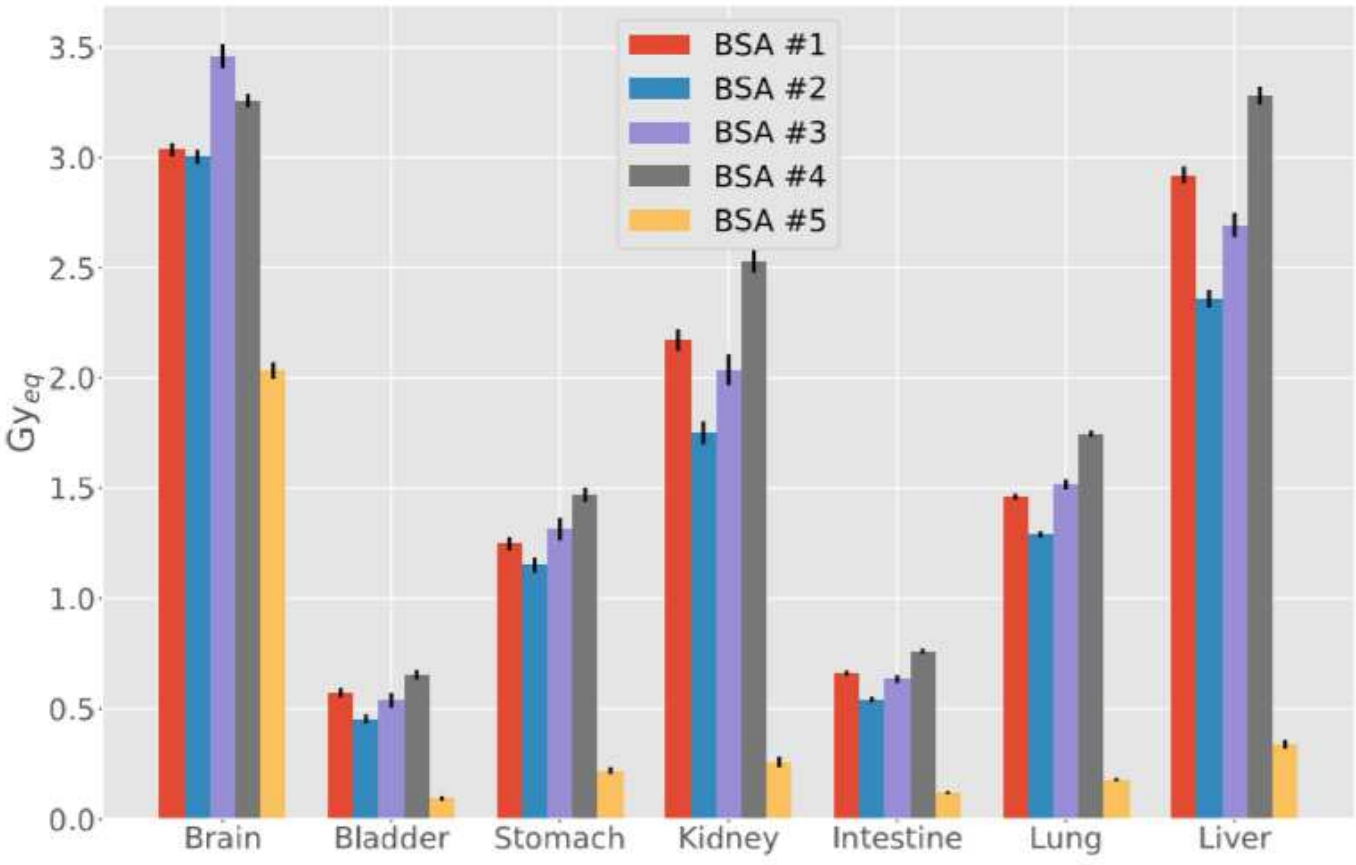

Figure 5

Comparison of out-of-beam dose evaluated in the MIRD phantom. Dose is evaluated for the treatment time, which is: 10 minutes for BSA #1, 12.5 minutes for BSA #2, 20 minutes for BSA #3, 9.5 minutes for BSA #4 and 24.5 minutes for BSA #5.

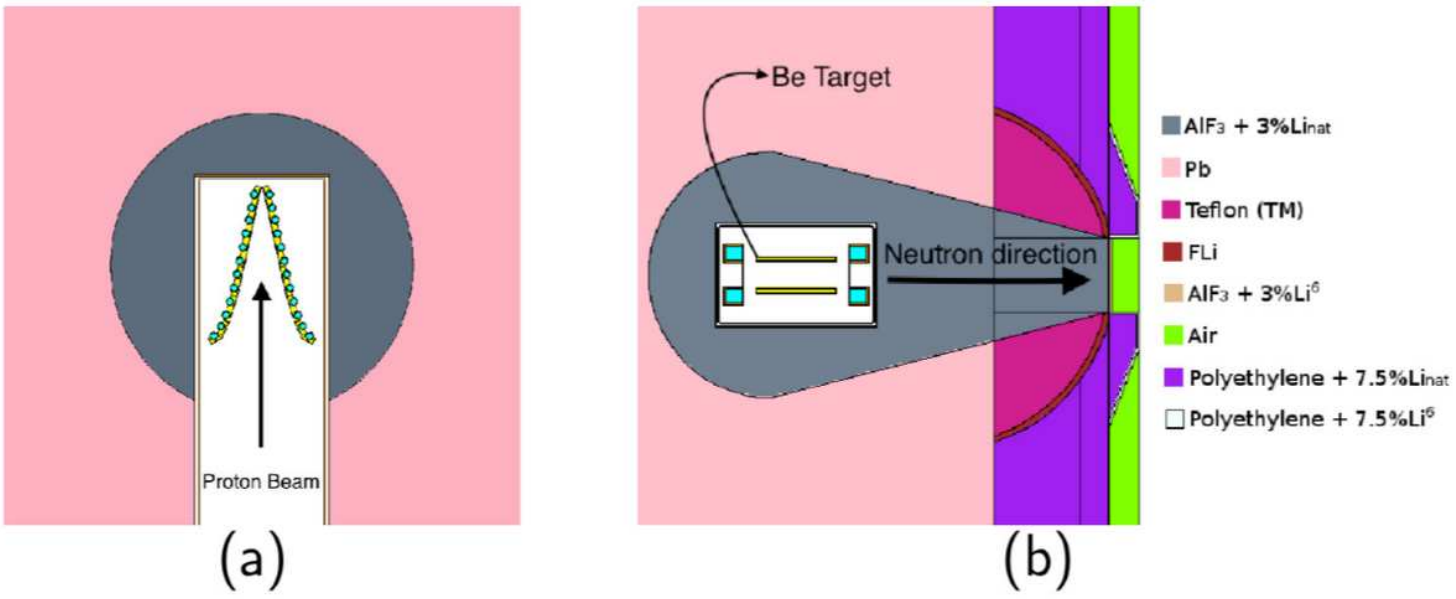

Figure 6

Geometrical configuration of the final BSA, the different colours represent the material composition of the BSA. Left: xy plane: the proton beam hits the target in the z direction. Right: xz plane. The target has a V-shape, to keep a compact design while removing the total heat generated [14].

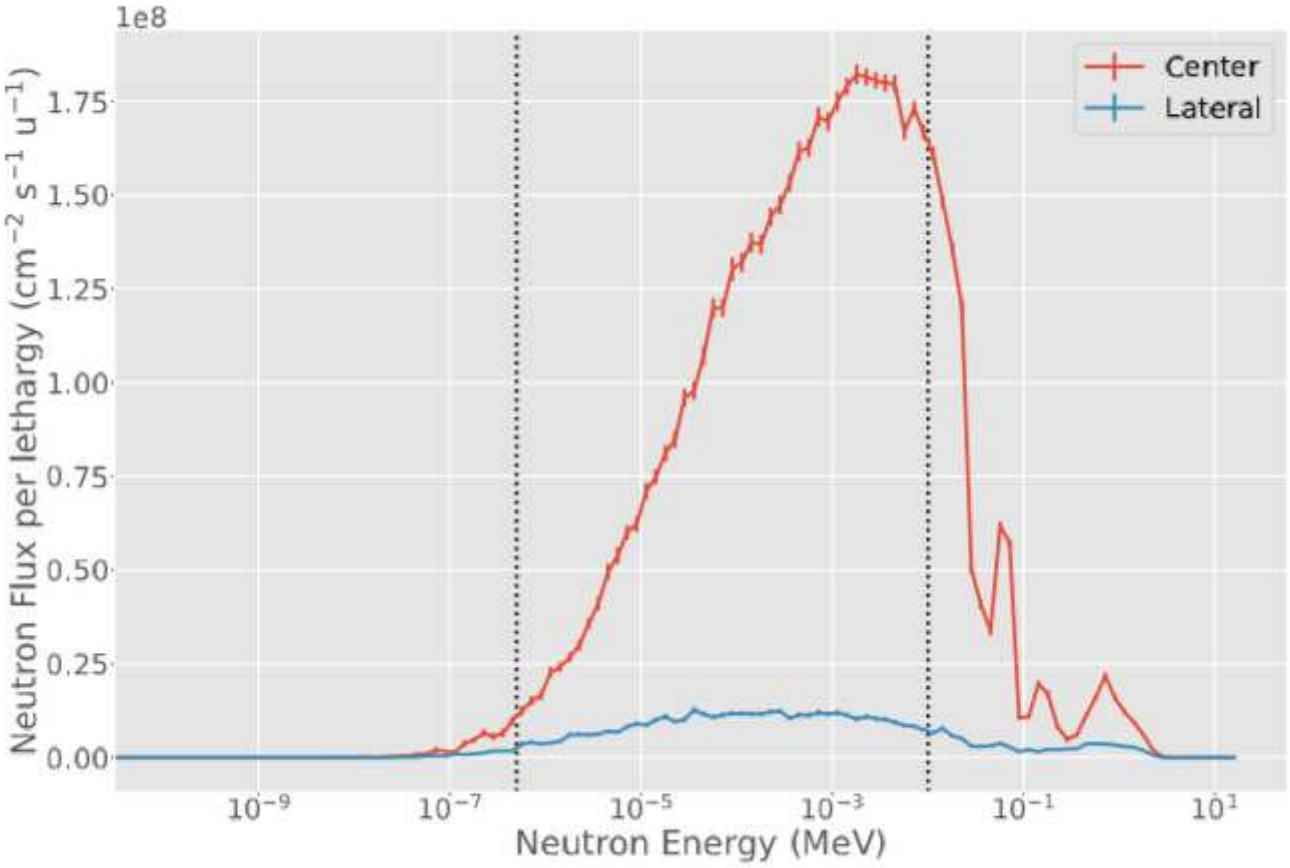

Figure 7

Final BSA energy spectra at the surface of the beam-port. Blue line: energy spectrum in a 6 cm radius disk, corresponding to the beam-port. Yellow line: spectrum in a ring with minimum radius of 6 cm and maximum radius of 12 cm. The two vertical dotted lines separate thermal from epithermal energy ranges (5· 10−7 MeV) and epithermal from fast energy ranges (10−2 MeV).

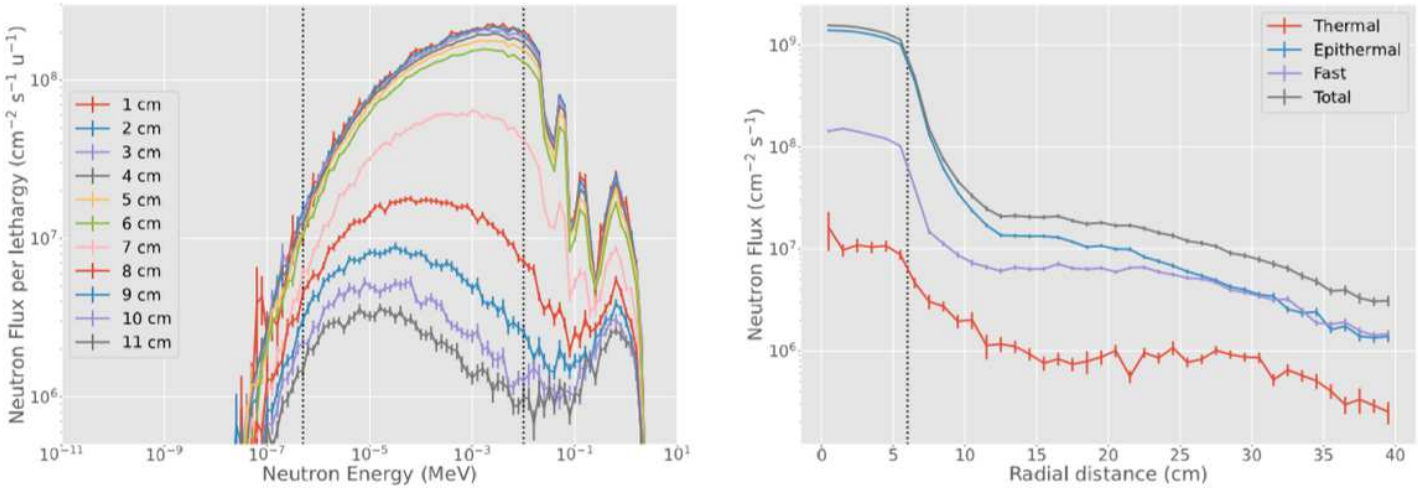

Figure 8

Neutron flux and energy spectra at the beam-port for BSA #5. a) neutron spectra in concentric rings, with radii increasing by 1 cm. The two vertical dotted lines separate thermal from epithermal energy ranges (5· 10−7 MeV) and epithermal from fast energy ranges (10−2 MeV). b) radial neutron flux distribution from the centre of the beam-port in concentric rings going from 0 cm to 40 cm of radius. The vertical dotted line delimits the beam-port radius. Blue: thermal neutron flux (E ≤ 5· 10−7 MeV), orange: epithermal flux (5· 10−7 MeV < E ≤10−2 MeV), green: fast flux (10−2 MeV < E) and red: total neutron flux.

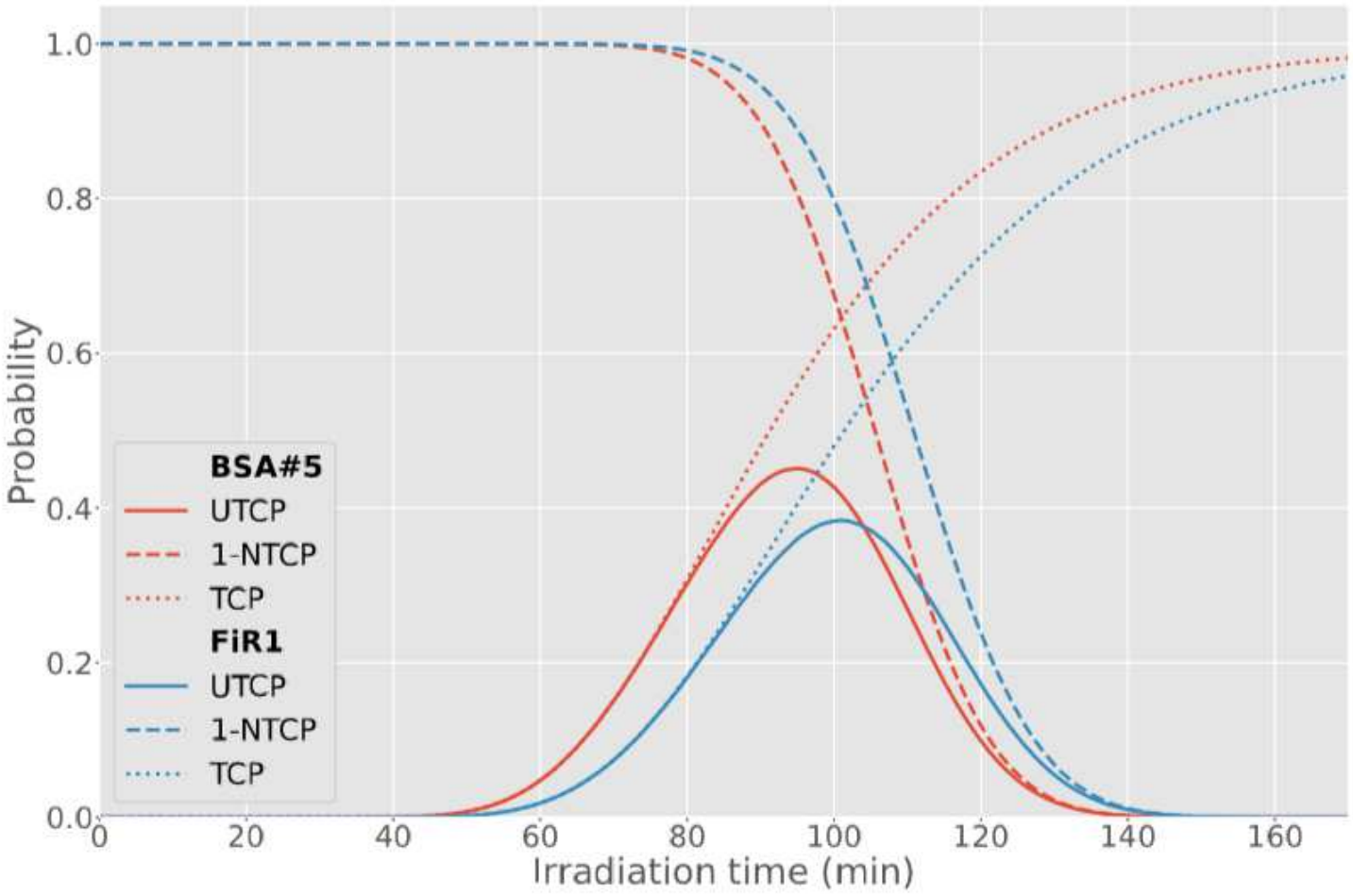

Figure 9

Comparison of the UTCP value for BSA #5 and FiR 1 as a function of the irradiation time.

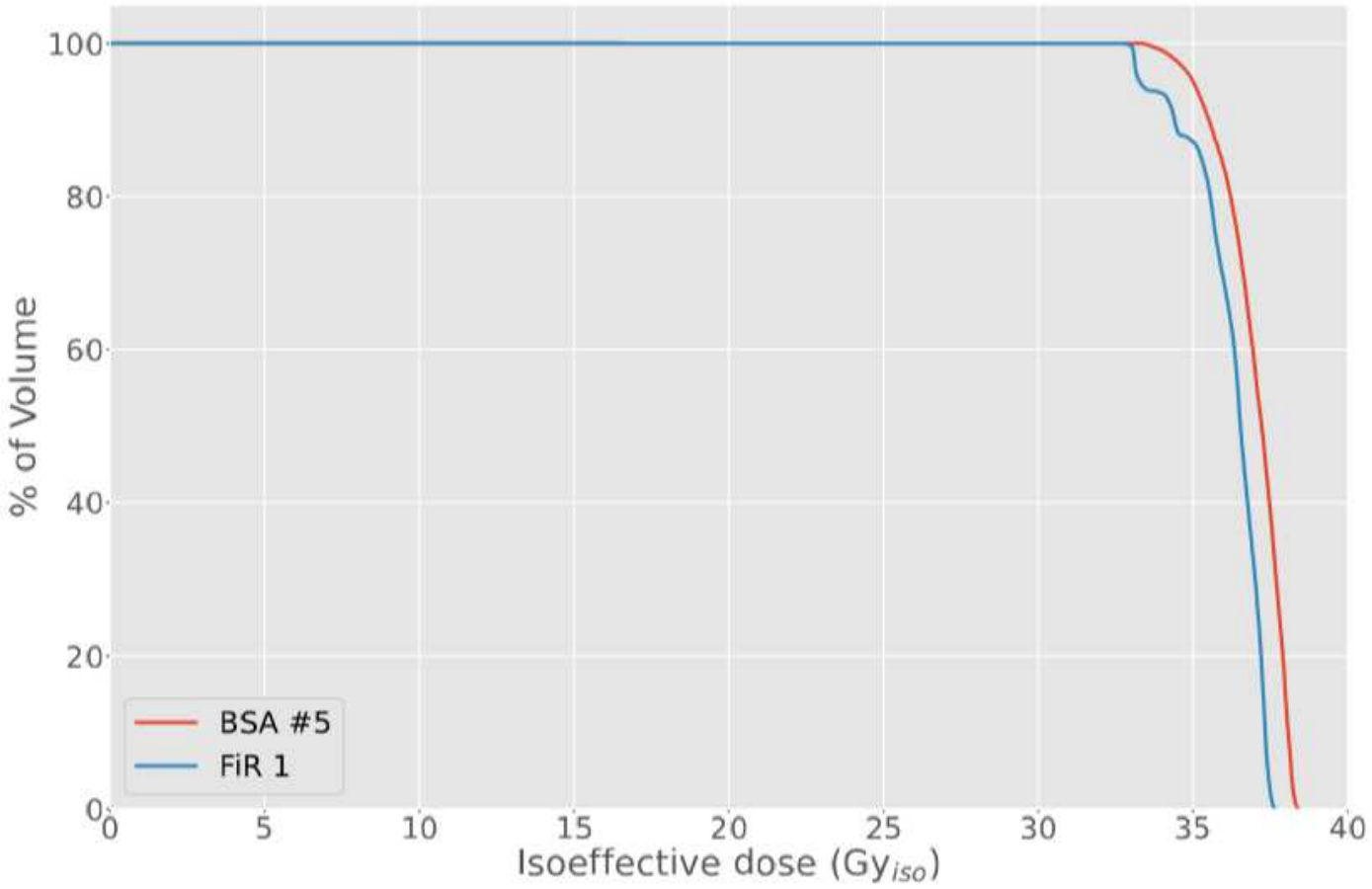

Figure 10

Comparison of the DVH obtained with BSA #5 and FiR 1.

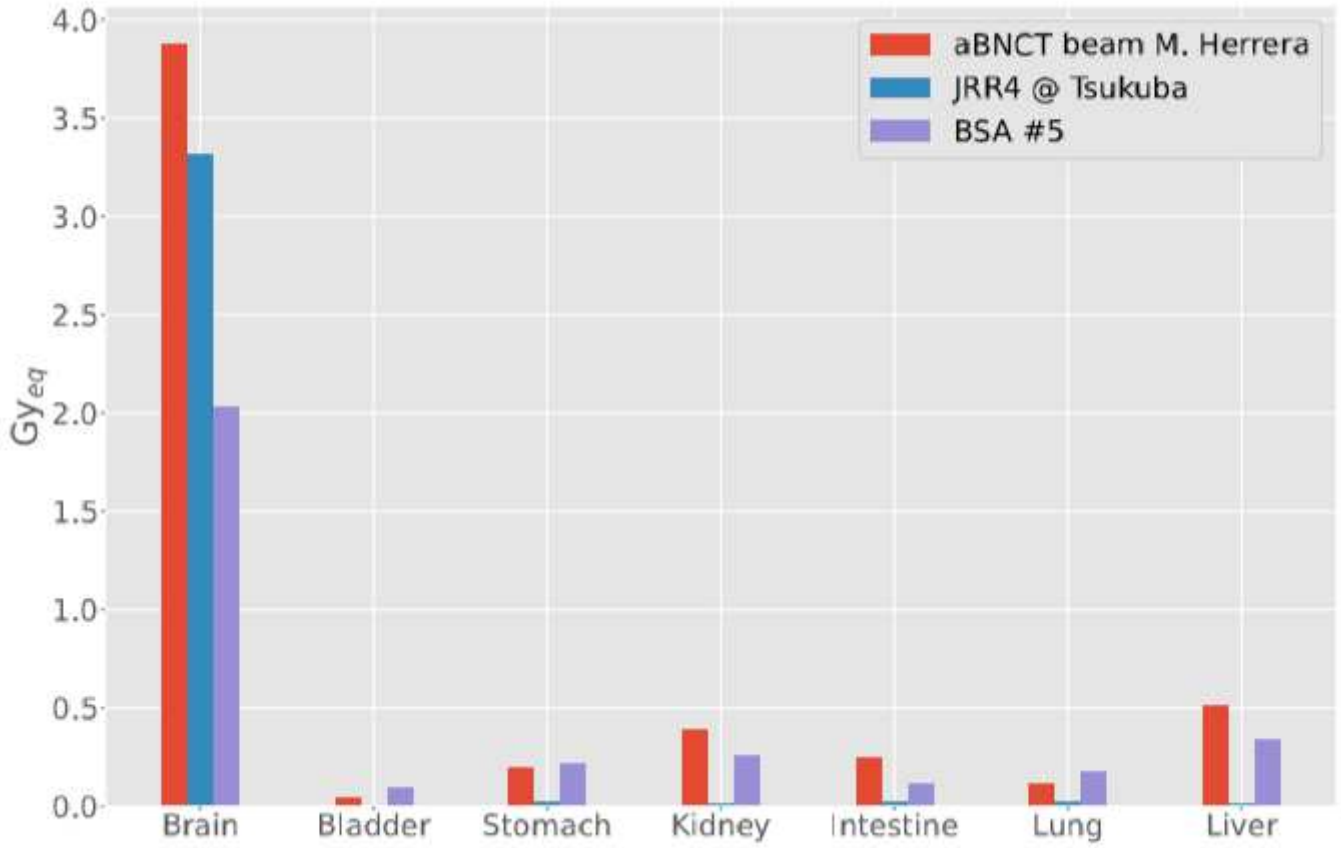

Figure 11

Out-of-beam dose evaluated in the MIRD phantom with BSA #5, with a clinical reactor beam (JRR4) and with the ab-BNCT neutron beam designed by Herrera starting for 2.7 MeV protons coupled with Li target [49].